MCAM controls cell autonomous polarity in myogenic and chondrogenic differentiation

Artal Moreno-Fortuny[#], Laricia Bragg[#], Giulio Cossu, Urmas Roostalu[1]

Manchester Academic Health Science Centre, Division of Extracellular Matrix and Regenerative Medicine, Faculty of Biology, Medicine and Health, University of Manchester, UK

[#]Equal contribution

[1]Correspondence: urmas@roostalu.info

ABSTRACT

Cell polarity has a fundamental role in shaping the morphology of cells and growing tissues. Polarity is commonly thought to be established in response to extracellular signals. Here we show that cell polarity forms in the absence of morphogen gradients in chondrogenic and myogenic differentiation. We demonstrate a key role for melanoma cell adhesion molecule (MCAM) in the initiation of cell polarity. We found highly polarized localization of MCAM, Moesin (MSN), Scribble (SCRIB) and Van-Gogh-like 2 (VANGL2) at the distal end of elongating myotubes. Knockout of MCAM or elimination of its endocytosis motif does not impair the initiation of myogenesis or myoblast fusion, but prevents myotube elongation. MSN, SCRIB and VANGL2 remain uniformly distributed in MCAM knockout cells. We show that MCAM dependent cell polarity is required at early stages of chondrogenic differentiation. In both myogenic and chondrogenic differentiation MCAM knockout leads to transcriptional downregulation of *Scrib* and enhanced MAP kinase activity. Our data demonstrates the importance of cell autonomous polarity in differentiation.

KEY WORDS: cell polarity, MCAM, myogenesis, chondrogenesis, differentiation

INTRODUCTION

Determination of cell polarity is one of the core principles in developmental biology (Leung et al., 2016). Experiments in model organisms, ranging from the fruit fly to mouse, have demonstrated how cell polarity and differentiation are influenced by morphogen gradients and local tissue architecture (Heller and Fuchs, 2015; Lawrence and Casal, 2013; Lawrence et al., 2007). However, an important question has remained unanswered – how differentiating cells achieve polarity in the absence of external signals? An example here is the skeletal muscle cell that even *in vitro* elongates in a highly polarized orientation.

The principal known mechanism underlying the initiation of cell polarity relies on non-canonical WNT signalling. WNT activity leads to Dishevelled (DVL) activation, reorganization of cytoskeleton and phosphorylation of C-JUN transcription factor (Devenport, 2014; Gomez-Orte et al., 2013; Niehrs, 2012). The apical-basal polarity is eventually established by an intricate network of positive and negative regulatory interactions. Loss of apical SCRIB polarity complex leads to the expansion of basolateral PAR3-PAR6-aPKC complex (Bilder and Perrimon, 2000; Bilder et al., 2003). Much of our current knowledge about cell polarity arises from research in invertebrate models and only a few studies have addressed its role in vertebrate mesoderm development. It has been shown how in embryonic development neural tube secreted WNT11 acts as a morphogen to direct myotube elongation via activation of the planar cell polarity pathway (Gros et al., 2009). In adult skeletal muscle cell polarity regulates the asymmetric division of satellite cells (Le Grand et al., 2009; Ono et al., 2015). Cell polarity guides also chondrocyte proliferation in the elongation of long bones (Gao et al., 2011; Li and Dudley, 2009; Wang et al., 2011).

In migrating melanoma cells non-canonical WNT signalling leads to cytoskeletal rearrangement and asymmetric distribution of MCAM (CD146) through its controlled endocytosis (Witze et al., 2008). The importance of MCAM in regulating cell polarity has however remained unknown. MCAM is highly expressed in embryonic development and is maintained in postnatal skeletal muscle satellite cells and osteogenic mesenchymal stromal cells (Alexander et al., 2016; Chan et al., 2005; Li et al.,

2003; Pujades et al., 2002; Sacchetti et al., 2007; Shi and Gronthos, 2003; Shih and Kurman, 1996). It is prominently upregulated in metastatic tumours (Johnson et al., 1996; Wang and Yan, 2013). Despite its wide-spread expression in developing tissues little is known about its role in cellular differentiation. Here we show that MCAM controls the initiation of cell autonomous polarity in myogenic and osteochondrogenic differentiation *in vitro* in the absence of morphogen gradients. MCAM knockout or deletion of its endocytosis motif leads to loss of cell polarity and impaired differentiation.

RESULTS AND DISCUSSION

Generation and initial characterization of MCAM mutant cell lines

We sought a model that would enable us to follow cellular differentiation *in vitro* from the onset of fate commitment to terminal differentiation. We chose the multipotent embryonic 10T1/2 cells as these can be induced to acquire chondrogenic fate by recombinant BMP2 (Denker et al., 1999; Shea et al., 2003) and to myogenic fate by exposing them to testosterone after initial brief culture with 5-azacytidine (Singh et al., 2003). We used CRISPR/Cas9 mediated genome editing, followed by FACS and single-cell cloning to generate 3 cell lines (Fig. 1A). Lines C149 and C164 were made by targeting the second exon of *Mcam* (Fig. S1A-B). Given that the 10T1/2 genome is diploid, both lines carry two independent mutations. C149 line has a single basepair (bp) insertion c.106_107insA and a 2 bp insertion c.106_107insCG. Both mutations lead to change of amino acid (aa) code after position 35 and STOP codon after 88 or 66 aa respectively. Line C164 has a 4 bp deletion c.103_106delCCCG and a 1 bp insertion c.106_107insT, resulting in aa code change after position 34 and 35 respectively and STOP codon after 64 and 88 aa. The MCAM protein (648 aa long) has a C-terminal endocytosis motif at aa 643-646 and since endocytosis has been proposed to regulate MCAM trafficking in cell migration (Witze et al., 2008) we generated a third line, U125, that carries three mutations that all lead to the specific elimination of the endocytosis motif. Single bp mutation c.1899delG causes a frameshift that replaces the last 15 aa; c.1890-1908delCGGTGACAAGAGGGCTCCA affects the last

19 aa; and a larger 56 bp deletion starting from cDNA position c.1878 and encompassing 16 bp of the following intron replaces the last 22 aa of MCAM.

Western blot analysis and immunohistochemistry proved the absence of MCAM in lines C149 and C164, whereas U125 cells had MCAM expression similar to 10T1/2 cells (Fig. 1B-D). *Mcam* expression was upregulated in 10T1/2 and U125 cells upon differentiation, when either testosterone or BMP2 was added to the culture medium (Fig. 1B-D). In their undifferentiated state the morphology of MCAM knockout cells did not differ from unedited 10T1/2 cells (Fig. 1E). Therefore MCAM is largely dispensable for fibroblasts, making our system suitable for studying its role in the context of differentiation.

MCAM is required for chondrogenic and myogenic differentiation *in vitro*

BMP2 exposure led to chondrogenic differentiation of 10T1/2 cells by 4 days in culture, which was evident in intense alcian blue staining (Fig. 2A, S2A) and upregulation of chondrogenic transcription factor *Sox9* (Fig. 2C) (Bi et al., 1999). Knockout of MCAM abolished chondrogenic differentiation in all the established cell lines. Wild-type BMP2 treated cells progressed to osteogenesis by the 7th day in culture. Alkaline phosphatase positive osteogenic nodules formed (Fig. 2B) and terminal differentiation markers osteomodulin (*Omd*) and *Col10a1* were upregulated (Fig. 2D-E). Osteogenic differentiation was significantly impaired in the absence of MCAM. We could detect only weak induction of *Col10a1* by the 7th day (Fig. 2E).

In myogenic promoting conditions early transcriptional regulators *Myod1* and myogenin (*Myog)* were induced in both 10T1/2 and *Mcam* mutant cells after 4 days exposure to testosterone (Fig. 2F, H-I, S2B-C). Despite this seemingly unaffected initiation of the myogenic program, terminal differentiation into multinucleated myotubes was severely impaired in cells lacking MCAM or its endocytosis motif. MCAM mutant cells fused into multinucleated myogenic cells that failed to elongate (Fig. 2G, S2D). There was a correspondingly reduced expression of myosin heavy chain in *Mcam* mutant cell lines (Fig. 2J). These data show the importance of MCAM in regulating

mesodermal differentiation. Our results also highlight the differences between the role of MCAM in chondrogenic and myogenic commitment, whereby it is essential at the onset of the former, but not until the elongation stage in the latter.

Asymmetric distribution of MCAM controls cell autonomous polarity

We next addressed the molecular mechanisms by which MCAM controls differentiation. First we approached the established signalling pathways downstream of MCAM: it is known to induce DVL2 and C-JUN phosphorylation in cancer cells and its knockdown leads to the induction of canonical WNT pathway (Ye et al., 2013). We noticed increased C-JUN phosphorylation under both osteochondrogenic and myogenic conditions, but this occurred even in the absence of MCAM (Fig. 3A). DVL2 activity decreases in myogenesis (Yamaguchi et al., 2012) and we confirmed this here, however there were no consistent differences between wild-type and MCAM mutant cell lines (Fig. 3B). We did not detect significant changes in the expression of canonical WNT transcription factors T-cell factor 4 (*Tcf4)* and Lymphoid Enhancer Binding Factor 1 (*Lef1)* (Fig. S3A). Neither did we observe nuclear translocation of β-catenin or change in WNT5A staining (Fig. S3B-C). In cancer cells MCAM has been linked with *Id1* expression (Zigler et al., 2011), which is a known inhibitor of myogenesis (Jen et al., 1992). However, we did not detect altered *Id1* expression in MCAM mutant cell lines, indicating that this pathway is unlikely to explain defective myogenic differentiation (Fig. 3C). Overall these results led us to conclude that MCAM function in the context of differentiation is largely different from its role in migrating tumour cells.

Several lines of evidence link MCAM with actin cytoskeleton. It interacts directly with actin binding proteins hShroom1 (Dye et al., 2009) and MSN (Luo et al., 2012). We tested the phosphorylation levels of MSN, but detected only a small decrease in its activity in MCAM mutant cell lines (Fig. 3D). We found significant morphological changes in MCAM mutant cells, which are clearly visible in cytoskeletal organization (Fig. 3E). Most notably, myoblasts fused together into multinucleated cells that however expanded in size without elongating. This led us to hypothesize that myotube elongation

relies on cell autonomous initiation of polarity and defects in this process may underlie the phenotype seen in MCAM mutant cells. Furthermore, MSN is a known regulator cytoskeletal organization in cell polarity (Fehon et al., 2010; Polesello et al., 2002). Abnormal localization of polarity complex rather than large changes in its activity may therefore lead to the observed differentiation defects. We thus analysed whether MCAM and MSN are asymmetrically distributed in differentiating cells. We found that in elongating myotubes MCAM colocalizes with MSN at the distal tip of the cell (Fig. 3F-F'). We detected asymmetric distribution of MCAM also *in vivo*, in E17.5 mouse forelimb developing myotubes (Fig. 3G). Polarity in chondrogenic differentiation remains less obvious, although we could detect MCAM and MSN colocalization in 10T1/2 cells exposed to BMP2 (Fig. 3H). To analyse the *in vivo* relevance of this pathway we analysed mouse ear elastic cartilage and found highly polarized distribution of MCAM in SOX9 expressing chondrocytes (Fig. 3I-I').

We next analysed the localization of diverse polarity complex proteins in MCAM mutant cell lines in comparison to wild type cells undergoing myogenic differentiation. Similarly to MSN and MCAM we found highly asymmetric distribution of VANGL2 at the distal tips of elongating myotubes (Fig. 4A-B, S4A). Remarkably, in MCAM knockout cells such polarity was not established and MSN labelled the whole plasma membrane, whereas VANGL2 was uniformly distributed across the cell. We also detected colocalization of SCRIB with MCAM at the tip of an elongating myotube (Fig. 4D). Knockout of MCAM led to uniform distribution of SCRIB (Fig. 4E) and importantly, also its transcriptional downregulation (Fig. 4H). SCRIB gene regulatory elements have remained uncharacterized and the precise transcriptional link remains to be established. Intriguingly, elimination of MCAM endocytosis motif led to frequent localization of SCRIB on actin filaments (Fig. S4B-B''). SCRIB trafficking to cortical actin was recently established to rely on β spectrin (Boeda and Etienne-Manneville, 2015). Our data suggests that MCAM participates in SCRIB trafficking possibly by co-endocytosis.

Since SCRIB complex antagonizes cell cortex targeting of PAR3, we analysed its localization and found that in wild type cells PAR3 was largely cytoplasmic, whereas in MCAM mutant myotubes it was frequently enriched at the membrane (Fig. 4F-G). Also in MCAM endocytosis motif mutant cells,

VANGL2 and PAR3 were mislocalized (Fig. 4I). We conclude that subcellular trafficking of MCAM is important in the establishment of cell autonomous polarity in myogenic differentiation.

We also found significant downregulation of *Scrib* in MCAM mutant cell lines in chondrogenic differentiation (Fig. 4H). Intriguingly, while in wild type BMP2 exposed cells VANGL2 showed only limited asymmetric localization, in the absence of MCAM it accumulated across the cytoplasm (Fig. 4J). We could also detect membrane targeting of PAR3 in MCAM mutant cells, although it remained less prominent than in myogenic differentiation. We propose that cell polarity has a more dynamic role in chondrogenic differentiation. This explanation agrees with the established transient activity of planar cell polarity in growth plate chondrocytes, where it regulates the division plane of proliferating cells (Li and Dudley, 2009).

Several signalling pathways are regulated by cell polarity. Loss of SCRIB leads to enhanced MAP kinase pathway (ERK1/2) activity (Nagasaka et al., 2010) and since tight control over ERK1/2 signalling is required in chondrogenesis (Bobick and Kulyk, 2004) we tested its activity in MCAM mutant cell lines. While in both chondrogenic and myogenic differentiation wild type cells downregulate ERK1/2 phosphorylation, in MCAM mutant cells their levels remained as high as in undifferentiated cells, providing a mechanistic insight into signalling changes in the cells.

We have shown here that cell polarity can arise independently of external signals in myogenic and chondrogenic differentiation. We propose that highly asymmetric localization of MCAM recruits actin binding protein MSN, which is required for correct localization of SCRIB polarity complex. This model may explain how cell polarity and distinct morphology can arise in tissues such as skeletal muscle and cartilage where, due to high density and consequent poor penetrance, morphogen gradients are difficult to be established. Still, it is likely that local environment may have an impact on the cell autonomous polarity mechanism. Our data provides the first explanation on how myotubes achieve directed elongation *in vitro*. Highly polarized localization of MCAM and MSN together with other cell polarity regulators is needed for directed cytoskeletal organization and elongation of the multinucleated cell. We show that lack of MCAM and consequent downregulation of *Scrib* expression

are sufficient to prevent chondrogenic differentiation *in vitro*. Intriguingly, mice deficient of MCAM or MSN do not show significant developmental defects, albeit in both models abnormalities have been observed in postnatal pathological conditions (Doi et al., 1999; Jouve et al., 2015; Okayama et al., 2008; Tu et al., 2013; Zeng et al., 2014). ERM proteins (ezrin, radixin, MSN) show functional redundancy in most cell types, explaining the limited phenotype of MSN knockout mice (Fehon et al., 2010). It is likely that *in vivo* other proteins may compensate for the lack of MCAM, which is a broad spectrum cell surface receptor. The *in vitro* system has enabled us to establish its role in a minimal environment with limited ligands and adhesion substrates. Our data collectively demonstrate that cellular differentiation relies on an intrinsic, adhesion receptor dependent polarity mechanism.

ACKNOWLEDGEMENTS

U.R. was supported by BBSRC Anniversary Future Leader Fellowship (BB/M013170/1). G.C. was supported by BHF (PG/14/1/30549), MRC (MR/P016006/1), Duchenne Parent Project (Italy) and Fundació La Marató grants. We are grateful to M. C. Jackson for help with cell sorting and to A. Adamson for advice on genome editing.

AUTHOR CONTRIBUTIONS

A.M.F. conducted gene expression experiments and analysed data. L.B. carried out protein analysis. G.C. discussed results and contributed to the manuscript. U.R. designed the study, generated cell lines, conducted experiments, analysed data and prepared the manuscript.

CONFLICTS OF INTEREST

The authors declare no conflicts of interests regarding this manuscript.

MATERIALS AND METHODS

Genome editing

CRISPR-Cas9 guide RNAs were designed in Benchling software (Benchling, Inc.). For N-terminal mutations in cell lines C149 and C164 guide RNA GCCAGTACCCACGCCCGACC/**TGG** and for the C-terminal mutation in line U125 guide RNA GGGCAGCAACGGTGACAAGA/**GGG** was used (PAM sequence in bold). These guides were cloned into SpCas9(BB)-2A-GFP plasmid as previously described (Ran et al., 2013). pSpCas9(BB)-2A-GFP was a gift from Feng Zhang (Addgene plasmid # 48138). 10T1/2 cells were purchased from Public Health England and cultured in MEM (Gibco), supplemented with 1% L-Glut, 10% FBS, 1% PS, 1x MEM Non-Essential Amino Acids Solution. Cells were transfected with guide RNA containing plasmid using Lipofectamine 3000 (Thermo Scientific) and after 24 h culture the GFP expressing cells were sorted into 96 well plates by BD FACS Aria. Confluent wells were split to isolate genomic DNA. The guide RNAs were designed so that indels would destroy a restriction enzyme binding site (XcmI for N-terminal and BpmI for C-termina edit). The PCR product was further verified by Sanger sequencing and analysis using CRISPR-ID (Dehairs et al., 2016). Selected lines were confirmed by cloning PCR product and sequencing individual bacterial colonies. For differentiation assays cells were plated at a density of 3200/cm^2. Myogenic differentiation of 10T1/2 cells was carried out as described (Singh et al., 2003), by initial 3-day culture in 20 μM 5-Azacytidine (Sigma Aldrich, A2385), followed by 3 day recovery in growth medium and 4-7 day incubation with 100 nM testosterone. For chondrogenic differentiation cells were incubated with recombinant BMP2 (200 ng/ml, R&D, 355-BM-050) for 4-7 days.

Alcian blue and alkaline phosphatase staining

Alcian Blue staining was carried out by washing the sample 3×5 minutes in PBS supplemented with 0.1% Tween (PTW) and 2×5 minutes in 3% Acetic acid. Thereafter Alcian Blue (Sigma-Aldrich, 1% solution in 3% Acetic acid) was added to the sample for 30 minutes, after which it was washed off with 3% Acetic acid followed by 3 washed in PBS (5 minutes each). Alkaline phosphatase staining was carried out using Vector Laboratories Red AP kit.

Immunohistochemistry

Cells were grown on glass-bottom plates (24-well Sensoplate, Greiner Bio-One), washed with PBS and fixed in 4% paraformaldehyde for 10 minutes. The fixed cells were washed 3×5 minutes in PTW and incubated for 3 h in blocking buffer (10% donkey serum in PTW) and overnight with primary antibodies in blocking buffer. Second day the samples were washed 3×5 minutes and 3×30 minutes in PTW, incubated for 30 minutes in 1% BSA in PTW and for 2 h with secondary antibodies in PTW (room temperature). Following the removal of the secondary antibody the samples were washed 3×15 minutes in PTW and 3×15 minutes in PBS. Inverted Zeiss Axio Observer Z1 was used together with Zeiss Zen software. Leica SP5 confocal was used together with the Leica Application Suite software. Images were acquired at 2 times line average and 3-5 times frame average, using sequential scanning mode. Single focal planes are shown.

Western blot

Cell samples were aspirated of media, washed 3 times with cold PBS then placed onto ice. Cold lysis (RIPA) buffer was added and the cells were scraped into sterile, pre-cooled tubes. These were incubated (with rotation) for 30-60 min at 4°C. After incubation, the samples were centrifuged and supernatant removed to a new pre-cooled tube. Protein concentration of each sample was determined using a Bradford assay. 20 ng of each sample was reduced and ran on a 4-12% NuPage Novex precast gel, following the NuPage Denaturing Electrophoresis protocol. The gels were transferred onto nitrocellulose membranes following standard protocol. The membranes were blocked using either 5% non-fat milk or 5% BSA (for phosphorylation-specific antibodies) in TBS-Tween for 60-120 min at RT. Primary antibodies were added into the relevant blocking solution and membranes incubated overnight at 4°C. After incubation they were washed 3× with TBS-Tween. Secondary antibodies (in fresh blocking solution) were added to the membranes and incubated for 60-120 min at RT. They were washed 3× with TBS-Tween after incubation. HRP substrate was added to each membrane. Chemiluminescent film was exposed to the membrane and developed using an automatic processor, JP-33.

Antibodies

The antibodies were used at the following concentrations: Rat anti-MCAM (R&D MAB7718; ICC 1:100), Sheep anti-MCAM (R&D AF6106; WB 1:1000), Goat anti-WNT5A (R&D AF645; ICC 1:50), Rabbit anti-LEF1 (Cell Signalling 2230; 1:100), Mouse anti-MyoD1 (Dako Clone 5.8A; ICC 1:200), Mouse anti-MYOG (The Developmental Studies Hybridoma Bank F5D; ICC 1:2), Mouse anti-MYH (The Developmental Studies Hybridoma Bank MF20; ICC 1:2), Rabbit anti-C-JUN (Cell Signalling 9165; WB 1:500), Rabbit anti-Phospho-c-JUN (Ser73) (Cell Signalling 3270; WB 1:500), Goat anti-VCL (Santa Cruz sc-7649; WB 1:2000), Mouse anti-GAPDH (Abcam ab125247; WB 1:2000), Rabbit anti-DVL2 (Abcam ab22616; WB 1:1000), Rabbit anti-phospho-DVL2 (Abcam ab124933; WB 1:1000), Rabbit anti-MSN (Abcam ab52490; ICC 1:100, WB 1:5000), Rabbit anti-phospho-MSN (Abcam ab177943; WB 1:500), Goat anti-VANGL2 (Santa Cruz sc-46561; ICC 1:100), Rabbit anti-SCRIB (Biorbyt orb337106; ICC 1:200), Rabbit anti-PAR3 (Novus Biologicals NBP1-88861; ICC 1:200), Rabbit anti ERK1/2 (Cell Signaling 4695; WB 1:1000), Rabbit anti-phospho-ERK1/2 (Cell Signaling 4370; WB 1:2000), Phalloidin-488 (Thermo Fischer A12379, ICC 1:100). Abbreviations: ICC – Immunocytochemistry; WB – Western blot.

RNA isolation and RT-qPCR

RNA extraction was performed using TRIzol reagent following the standard manufacturer's procedure (Thermo Fisher Scientific). Once resuspended, RNA was quantified with Nanodrop 2000. After treatment with DNase a standardized amount of RNA was used for retro-transcritpiton using random hexamer primers (RevertAid First Strand cDNA Synthesis Kit Thermo Fisher Scientific, 1621). RT-qPCR was carried out using FastStart Essential DNA Master Mix (Roche) on a Roche LightCycler 96 system. RT-qPCRs were performed in triplicate for each sample and 3 biological replicates were used. Absolute quantification of each target was performed using a standard curved as a reference in Roche LightCycler software version 1.5. Primer sequences were acquired from Harvard PrimerBank (Spandidos et al., 2008; Spandidos et al., 2010; Wang and Seed, 2003): *Mcam* (10566955a1), *Gapdh* (6679937a1), *MyoD1* (6996932a1), *Myh2* (21489941a1), Sox9 (31543761a1),

Omd (6754934a1), *Col10a1* (6753480a1), *Scrib* (20373163a1), Lef1 (27735019a1), Tcf4 (7305551a1).

REFERENCES

Alexander, M. S., Rozkalne, A., Colletta, A., Spinazzola, J. M., Johnson, S., Rahimov, F., Meng, H., Lawlor, M. W., Estrella, E., Kunkel, L. M. et al. (2016). CD82 Is a Marker for Prospective Isolation of Human Muscle Satellite Cells and Is Linked to Muscular Dystrophies. *Cell stem cell* **19**, 800-807.

Bi, W., Deng, J. M., Zhang, Z., Behringer, R. R. and de Crombrugghe, B. (1999). Sox9 is required for cartilage formation. *Nature genetics* **22**, 85-9.

Bilder, D. and Perrimon, N. (2000). Localization of apical epithelial determinants by the basolateral PDZ protein Scribble. *Nature* **403**, 676-80.

Bilder, D., Schober, M. and Perrimon, N. (2003). Integrated activity of PDZ protein complexes regulates epithelial polarity. *Nature cell biology* **5**, 53-8.

Bobick, B. E. and Kulyk, W. M. (2004). The MEK-ERK signaling pathway is a negative regulator of cartilage-specific gene expression in embryonic limb mesenchyme. *The Journal of biological chemistry* **279**, 4588-95.

Boeda, B. and Etienne-Manneville, S. (2015). Spectrin binding motifs regulate Scribble cortical dynamics and polarity function. *Elife* **4**.

Chan, B., Sinha, S., Cho, D., Ramchandran, R. and Sukhatme, V. P. (2005). Critical roles of CD146 in zebrafish vascular development. *Developmental dynamics : an official publication of the American Association of Anatomists* **232**, 232-44.

Dehairs, J., Talebi, A., Cherifi, Y. and Swinnen, J. V. (2016). CRISP-ID: decoding CRISPR mediated indels by Sanger sequencing. *Sci Rep* **6**, 28973.

Denker, A. E., Haas, A. R., Nicoll, S. B. and Tuan, R. S. (1999). Chondrogenic differentiation of murine C3H10T1/2 multipotential mesenchymal cells: I. Stimulation by bone morphogenetic protein-2 in high-density micromass cultures. *Differentiation; research in biological diversity* **64**, 67-76.

Devenport, D. (2014). The cell biology of planar cell polarity. *The Journal of cell biology* **207**, 171-9.

Doi, Y., Itoh, M., Yonemura, S., Ishihara, S., Takano, H., Noda, T. and Tsukita, S. (1999). Normal development of mice and unimpaired cell adhesion/cell motility/actin-based cytoskeleton without compensatory up-regulation of ezrin or radixin in moesin gene knockout. *The Journal of biological chemistry* **274**, 2315-21.

Dye, D. E., Karlen, S., Rohrbach, B., Staub, O., Braathen, L. R., Eidne, K. A. and Coombe, D. R. (2009). hShroom1 links a membrane bound protein to the actin cytoskeleton. *Cell Mol Life Sci* **66**, 681-96.

Fehon, R. G., McClatchey, A. I. and Bretscher, A. (2010). Organizing the cell cortex: the role of ERM proteins. *Nature reviews. Molecular cell biology* **11**, 276-87.

Gao, B., Song, H., Bishop, K., Elliot, G., Garrett, L., English, M. A., Andre, P., Robinson, J., Sood, R., Minami, Y. et al. (2011). Wnt signaling gradients establish planar cell polarity by inducing Vangl2 phosphorylation through Ror2. *Developmental cell* **20**, 163-76.

Gomez-Orte, E., Saenz-Narciso, B., Moreno, S. and Cabello, J. (2013). Multiple functions of the noncanonical Wnt pathway. *Trends in genetics : TIG* **29**, 545-53.

Gros, J., Serralbo, O. and Marcelle, C. (2009). WNT11 acts as a directional cue to organize the elongation of early muscle fibres. *Nature* **457**, 589-93.

Heller, E. and Fuchs, E. (2015). Tissue patterning and cellular mechanics. *The Journal of cell biology* **211**, 219-31.

Jen, Y., Weintraub, H. and Benezra, R. (1992). Overexpression of Id protein inhibits the muscle differentiation program: in vivo association of Id with E2A proteins. *Genes & development* **6**, 1466-79.

Johnson, J. P., Rummel, M. M., Rothbacher, U. and Sers, C. (1996). MUC18: A cell adhesion molecule with a potential role in tumor growth and tumor cell dissemination. *Curr Top Microbiol Immunol* **213 (Pt 1)**, 95-105.

Jouve, N., Bachelier, R., Despoix, N., Blin, M. G., Matinzadeh, M. K., Poitevin, S., Aurrand-Lions, M., Fallague, K., Bardin, N., Blot-Chabaud, M. et al. (2015). CD146 mediates VEGF-induced melanoma cell extravasation through FAK activation. *Int J Cancer* **137**, 50-60.

Lawrence, P. A. and Casal, J. (2013). The mechanisms of planar cell polarity, growth and the Hippo pathway: some known unknowns. *Developmental biology* **377**, 1-8.

Lawrence, P. A., Struhl, G. and Casal, J. (2007). Planar cell polarity: one or two pathways? *Nat Rev Genet* **8**, 555-63.

Le Grand, F., Jones, A. E., Seale, V., Scime, A. and Rudnicki, M. A. (2009). Wnt7a activates the planar cell polarity pathway to drive the symmetric expansion of satellite stem cells. *Cell stem cell* **4**, 535-47.

Leung, C. Y., Zhu, M. and Zernicka-Goetz, M. (2016). Polarity in Cell-Fate Acquisition in the Early Mouse Embryo. *Current topics in developmental biology* **120**, 203-34.

Li, Q., Yu, Y., Bischoff, J., Mulliken, J. B. and Olsen, B. R. (2003). Differential expression of CD146 in tissues and endothelial cells derived from infantile haemangioma and normal human skin. *The Journal of pathology* **201**, 296-302.

Li, Y. and Dudley, A. T. (2009). Noncanonical frizzled signaling regulates cell polarity of growth plate chondrocytes. *Development* **136**, 1083-92.

Luo, Y., Zheng, C., Zhang, J., Lu, D., Zhuang, J., Xing, S., Feng, J., Yang, D. and Yan, X. (2012). Recognition of CD146 as an ERM-binding protein offers novel mechanisms for melanoma cell migration. *Oncogene* **31**, 306-21.

Nagasaka, K., Pim, D., Massimi, P., Thomas, M., Tomaic, V., Subbaiah, V. K., Kranjec, C., Nakagawa, S., Yano, T., Taketani, Y. et al. (2010). The cell polarity regulator hScrib controls ERK activation through a KIM site-dependent interaction. *Oncogene* **29**, 5311-21.

Niehrs, C. (2012). The complex world of WNT receptor signalling. *Nature reviews. Molecular cell biology* **13**, 767-79.

Okayama, T., Kikuchi, S., Ochiai, T., Ikoma, H., Kubota, T., Ichikawa, D., Fujiwara, H., Okamoto, K., Sakakura, C., Sonoyama, T. et al. (2008). Attenuated response to liver injury in moesin-deficient mice: impaired stellate cell migration and decreased fibrosis. *Biochimica et biophysica acta* **1782**, 542-8.

Ono, Y., Urata, Y., Goto, S., Nakagawa, S., Humbert, P. O., Li, T. S. and Zammit, P. S. (2015). Muscle stem cell fate is controlled by the cell-polarity protein Scrib. *Cell Rep* **10**, 1135-48.

Polesello, C., Delon, I., Valenti, P., Ferrer, P. and Payre, F. (2002). Dmoesin controls actin-based cell shape and polarity during Drosophila melanogaster oogenesis. *Nature cell biology* **4**, 782-9.

Pujades, C., Guez-Guez, B. and Dunon, D. (2002). Melanoma Cell Adhesion Molecule (MCAM) expression in the myogenic lineage during early chick embryonic development. *The International journal of developmental biology* **46**, 263-6.

Ran, F. A., Hsu, P. D., Wright, J., Agarwala, V., Scott, D. A. and Zhang, F. (2013). Genome engineering using the CRISPR-Cas9 system. *Nat Protoc* **8**, 2281-308.

Sacchetti, B., Funari, A., Michienzi, S., Di Cesare, S., Piersanti, S., Saggio, I., Tagliafico, E., Ferrari, S., Robey, P. G., Riminucci, M. et al. (2007). Self-renewing osteoprogenitors in bone marrow sinusoids can organize a hematopoietic microenvironment. *Cell* **131**, 324-36.

Shea, C. M., Edgar, C. M., Einhorn, T. A. and Gerstenfeld, L. C. (2003). BMP treatment of C3H10T1/2 mesenchymal stem cells induces both chondrogenesis and osteogenesis. *J Cell Biochem* **90**, 1112-27.

Shi, S. and Gronthos, S. (2003). Perivascular niche of postnatal mesenchymal stem cells in human bone marrow and dental pulp. *Journal of bone and mineral research : the official journal of the American Society for Bone and Mineral Research* **18**, 696-704.

Shih, I. M. and Kurman, R. J. (1996). Expression of melanoma cell adhesion molecule in intermediate trophoblast. *Lab Invest* **75**, 377-88.

Singh, R., Artaza, J. N., Taylor, W. E., Gonzalez-Cadavid, N. F. and Bhasin, S. (2003). Androgens stimulate myogenic differentiation and inhibit adipogenesis in C3H 10T1/2 pluripotent cells through an androgen receptor-mediated pathway. *Endocrinology* **144**, 5081-8.

Spandidos, A., Wang, X., Wang, H., Dragnev, S., Thurber, T. and Seed, B. (2008). A comprehensive collection of experimentally validated primers for Polymerase Chain Reaction quantitation of murine transcript abundance. *BMC Genomics* **9**, 633.

Spandidos, A., Wang, X., Wang, H. and Seed, B. (2010). PrimerBank: a resource of human and mouse PCR primer pairs for gene expression detection and quantification. *Nucleic acids research* **38**, D792-9.

Tu, T., Gao, Q., Luo, Y., Chen, J., Lu, D., Feng, J., Yang, D., Song, L. and Yan, X. (2013). CD146 deletion in the nervous system impairs appetite, locomotor activity and spatial learning in mice. *PloS one* **8**, e74124.

Wang, B., Sinha, T., Jiao, K., Serra, R. and Wang, J. (2011). Disruption of PCP signaling causes limb morphogenesis and skeletal defects and may underlie Robinow syndrome and brachydactyly type B. *Human molecular genetics* **20**, 271-85.

Wang, X. and Seed, B. (2003). A PCR primer bank for quantitative gene expression analysis. *Nucleic acids research* **31**, e154.

Wang, Z. and Yan, X. (2013). CD146, a multi-functional molecule beyond adhesion. *Cancer Lett* **330**, 150-62.

Witze, E. S., Litman, E. S., Argast, G. M., Moon, R. T. and Ahn, N. G. (2008). Wnt5a control of cell polarity and directional movement by polarized redistribution of adhesion receptors. *Science* **320**, 365-9.

Yamaguchi, Y., Naiki, T. and Irie, K. (2012). Stau1 regulates Dvl2 expression during myoblast differentiation. *Biochemical and biophysical research communications* **417**, 427-32.

Ye, Z., Zhang, C., Tu, T., Sun, M., Liu, D., Lu, D., Feng, J., Yang, D., Liu, F. and Yan, X. (2013). Wnt5a uses CD146 as a receptor to regulate cell motility and convergent extension. *Nature communications* **4**, 2803.

Zeng, Q., Wu, Z., Duan, H., Jiang, X., Tu, T., Lu, D., Luo, Y., Wang, P., Song, L., Feng, J. et al. (2014). Impaired tumor angiogenesis and VEGF-induced pathway in endothelial CD146 knockout mice. *Protein Cell* **5**, 445-56.

Zigler, M., Villares, G. J., Dobroff, A. S., Wang, H., Huang, L., Braeuer, R. R., Kamiya, T., Melnikova, V. O., Song, R., Friedman, R. et al. (2011). Expression of Id-1 is regulated by MCAM/MUC18: a missing link in melanoma progression. *Cancer research* **71**, 3494-504.

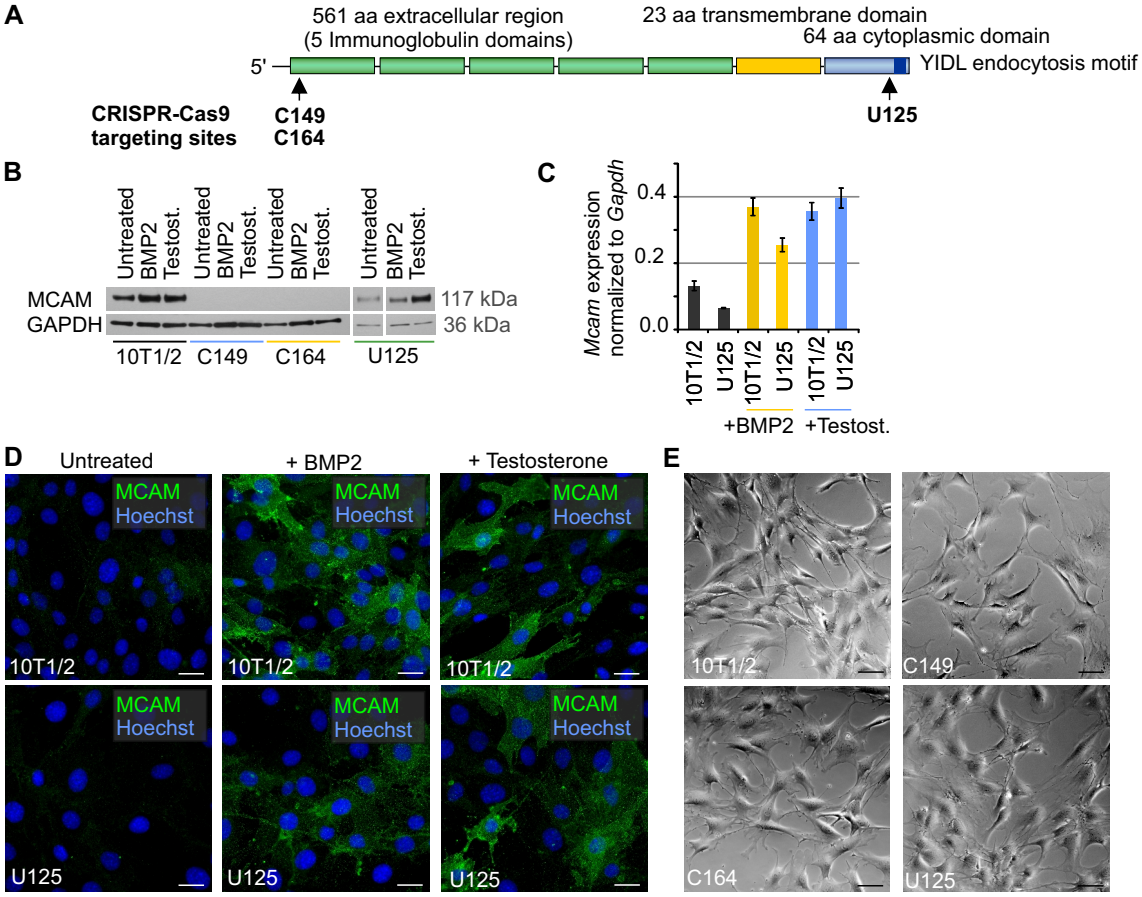

Fig. 1. Generation of MCAM knockout cell lines. (A) Schematic drawing of MCAM protein structure. CRISPR-Cas9 targeting regions for C149, C164 and U125 cell lines are indicated. (B) Western blot detection of MCAM in 10T1/2 cells undergoing osteochondrogenic (treated for 4 days with BMP2) or myogenic (treated for 4 days with testosterone) differentiation. U125 cells lack C-terminal endocytosis motif and express MCAM protein. GAPDH (Glyceraldehyde 3-phosphate dehydrogenase) – loading control. (C) RT-qPCR shows *Mcam* upregulation in 10T1/2 and U125 cells treated with either BMP2 or testosterone (mean +/- SEM). (D) Immunocytochemistry shows MCAM upregulation in differentiating 10T1/2 and U125 cells after four days with BMP2 or testosterone. (E) MCAM knockout or loss of its endocytosis motif did not change the morphology of naïve fibroblasts. Scale bars: 20 µm.

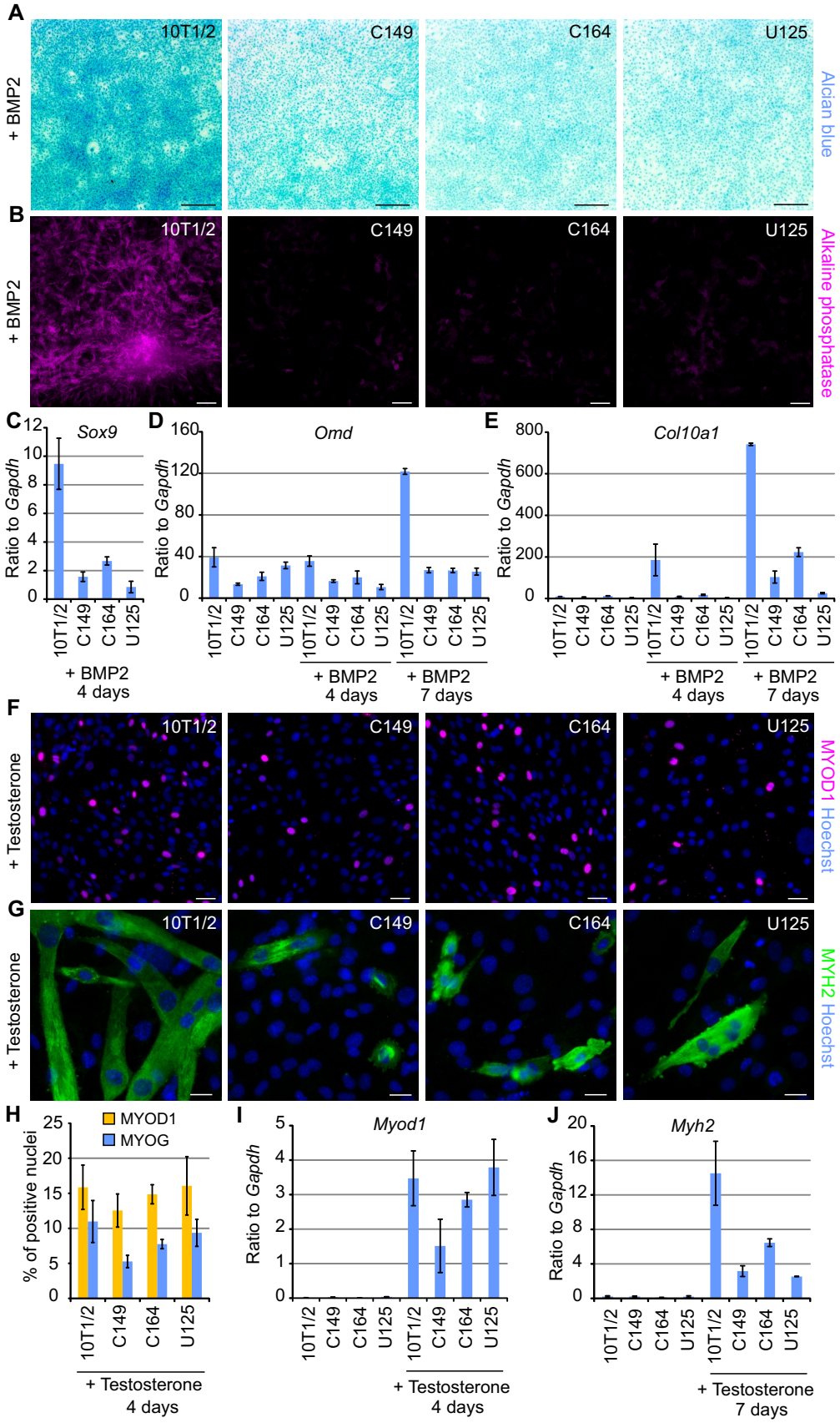

Fig. 2.

Fig. 2. Loss of MCAM function impairs chondrogenic and myogenic differentiation. (A) Alcian blue staining showing that in comparison to wild type 10T1/2 cells chondrogenic differentiation fails in MCAM mutant cells (C146, C164, U125) treated for 4 days with BMP2. (B) MCAM loss of function abolished the formation of alkaline phosphatase positive osteogenic nodules in cultures treated for 7 days with BMP2. RT-qPCR (mean +/- SEM) analysis revealed (C) no upregulation of *Sox9* and diminished expression of (D) *Omd* and (E) *Col10a1* in MCAM knockout cell lines treated with BMP2. (F) MCAM knockout did not prevent MYOD1 upregulation after 4 day treatment with testosterone. (G) 7 day exposure to testosterone triggered extensive formation of multinucleated myotubes in wild-type 10T1/2 cells, whereas MCAM knockout cells failed to elongate into myotubes. (H) Quantification of MYOD1 and myogenin (MYOG1) positive nuclei after 4 day exposure to testosterone. RT-qPCR analysis of (I) *MyoD1* expression showing testosterone induced upregulation in both wild type and MCAM knockout cells at 4 days, and (J) reduced expression of myosin heavy chain (*Myh2*) in *Mcam* mutant cells at 7 days. Scale bars: A, 500 µm; B, 200 µm; F, 50 µm; G, 20 µm.

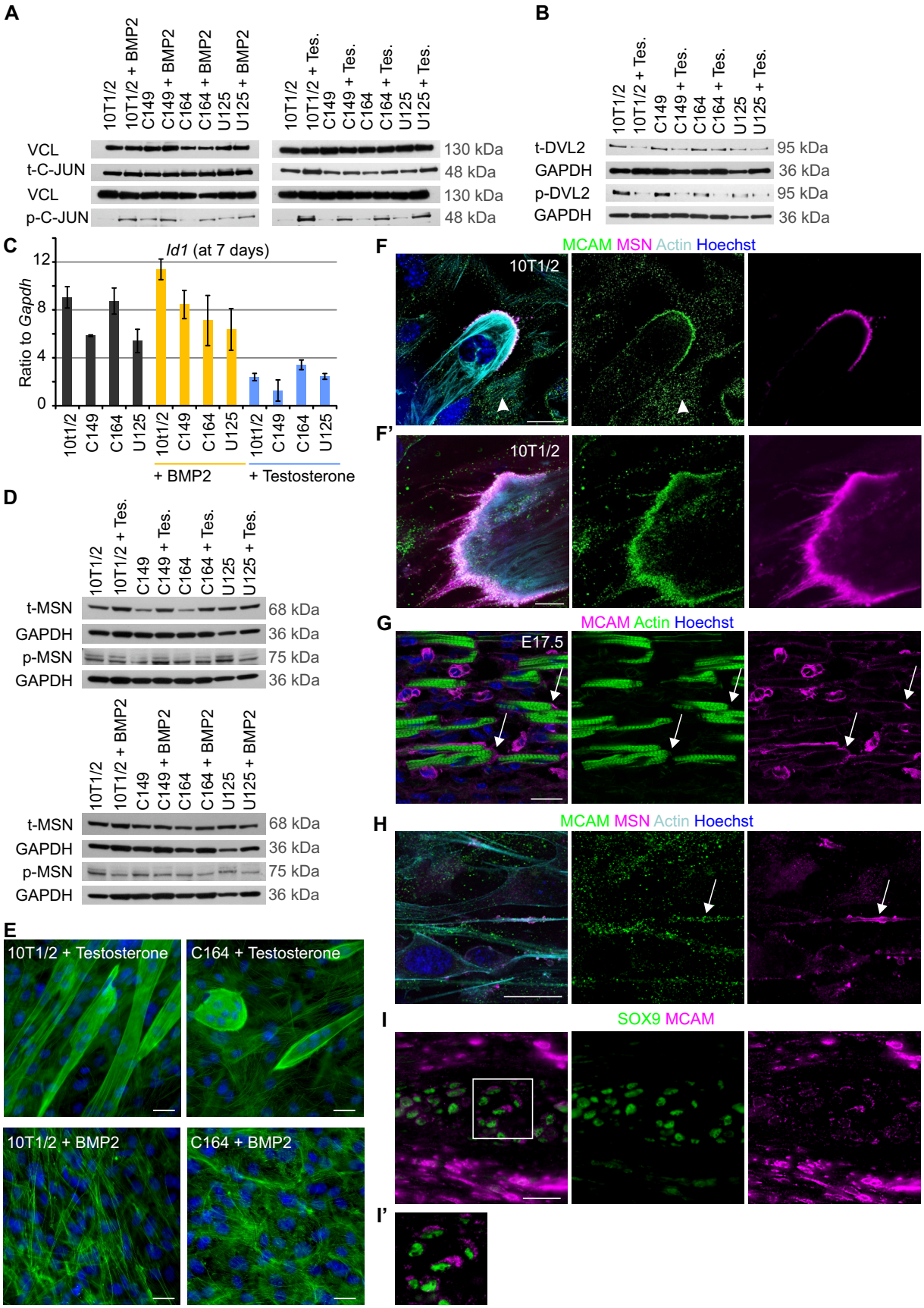

Fig. 3.

Fig. 3. Asymmetric distribution of MCAM and MSN in differentiating cells does not affect WNT signalling. (A) MCAM loss of function did not lead to changes in total C-JUN level (t-C-JUN). Differentiation induced phosphorylation of C-JUN (p-C-JUN), which occurred independently of MCAM. VCL (Vinculin) - loading control. (B) Myogenic differentiation led to downregulation of total DVL2 and its phosphorylated form (p-DVL2), yet this occurred regardless of MCAM activity. GAPDH – loading control. (C) RT-qPCR showing downregulation of *Id1* expression (mean +/- SEM) in cells undergoing myogenic differentiation. (D) Western blot analysis of total (t-) and phosphorylated (p-) MSN after 7 day exposure to BMP2 or testosterone. (E) Actin staining (Phalloidin-Alexa-488) illustrates large morphological changes in MCAM mutant cells. Multinucleated myotubes fail to elongate in the absence of MCAM (upper panel, 7 day treatment with testosterone) and chondrogenic cells show impaired cytoskeletal assembly (7 day exposure to BMP2). (F) In multinucleated myotubes MCAM colocalizes with MSN in the distal end of the cell, (F') often in cytoplasmic processes. In undifferentiated cells MCAM is primarily localized to cytoplasmic vesicles (arrowhead). (G) In foetal mouse limbs (E17.5) MCAM can be seen at ends of differentiating myofibres. (H) MCAM colocalizes with MSN also in 10T1/2 cells exposed for 7 days to BMP2. (I) Asymmetric distribution of MCAM in SOX9 labelled mouse ear elastic cartilage chondrocytes. (I') Magnification of the boxed area. Scale bars: E-F, G-I, 25 µm; F', 10 µm.

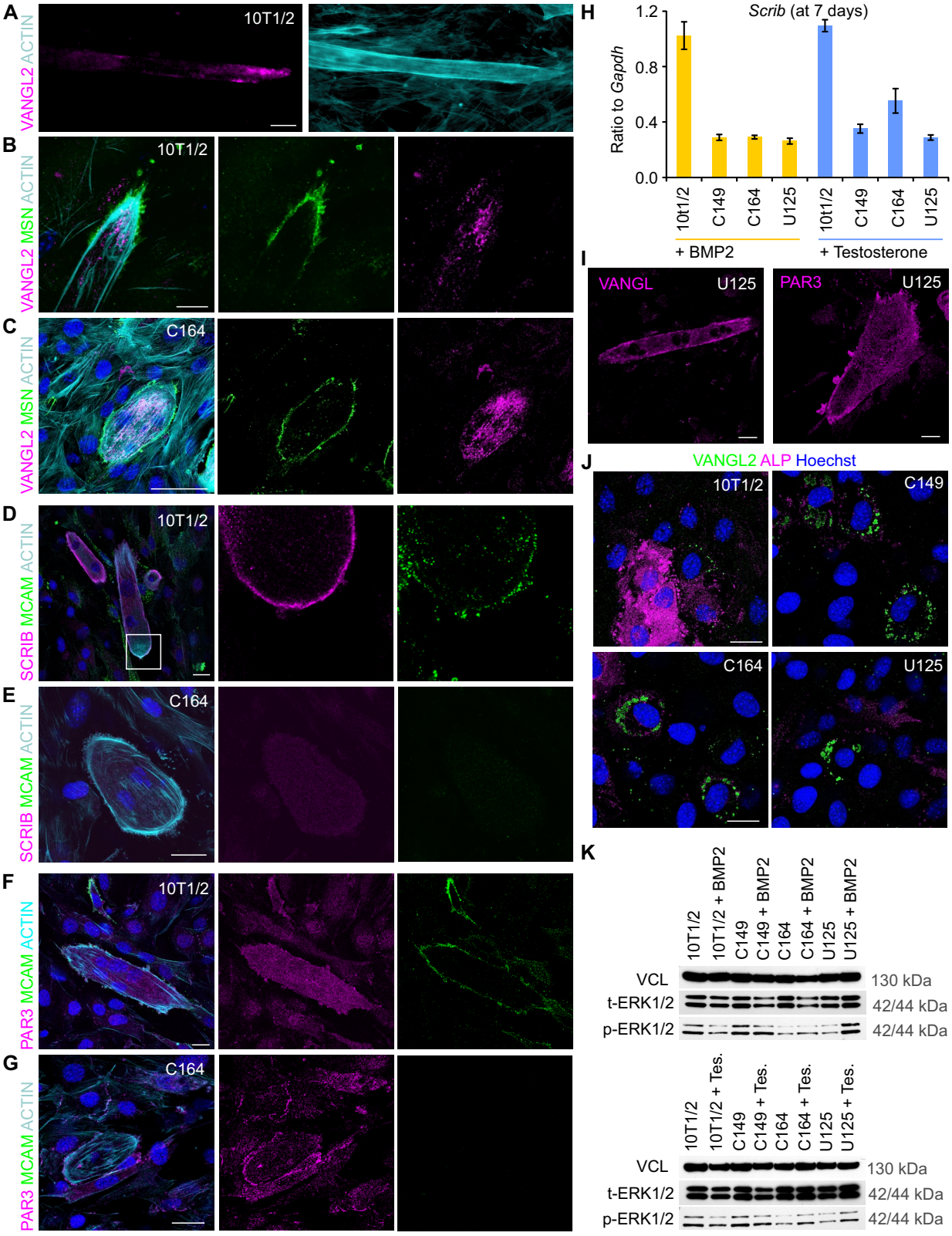

Fig. 4

Fig. 4. MCAM is required to establish cell autonomous polarity. (A) In elongating myotubes (10T1/2 cells treated with testosterone for 7 days) VANGL2 is localized asymmetrically at the tip of the cell. (B) The VANGL2 enriched tip of the cell is marked by MSN. (C) In MCAM knockout C164 cells myotube elongation fails, MSN labels the whole plasma membrane and VANGL2 is spread across the cytoplasm. (D) Highly polarized localization of MCAM and SCRIB at the distal end of growing wild type myotube. (E) In MCAM knockout cells SCRIB levels remain low and it is spread evenly in the cell. (F) In wild type myotubes PAR3 remains cytoplasmic, whereas (G) in MCAM knockout C164 cells it can be detected at the cell cortex. (H) RT-qPCR demonstrates reduced expression of *Scrib* in MCAM mutant cell lines. Cells were treated for 7 days with BMP2 or testosterone. (I) Deletion of MCAM endocytosis motif leads to similar polarity defects as complete MCAM elimination. VANGL2 is evenly spread in U125 cells and PAR3 accumulates in cell cortex. (J) In chondrogenic differentiation VANGL2 was observed asymmetrically in limited number of cells. In MCAM mutant cell lines (C149, C164, U125) VANGL2 accumulated around the nucleus. (K) Initiation of myogenic (4 day culture with testosterone) and chondrogenic differentiation (4 day culture with BMP2) led to downregulation of ERK1/2 phosphorylation (p-ERK1/2). Instead in MCAM mutant cell lines ERK1/2 phosphorylation increased. Scale bars: 25 μm.